Digital Analysis of Thermal Infrared Imagery using Temperature Mapping

Cheruku Venkateswarlu
Infosys Technologies Ltd.,
India
Venkateswarlu_C@infosys.com

Sumanth Yenduri
Louisiana State University
Baton Rouge, USA
sumanth@bit.csc.lsu.edu

S.S. Iyengar
Louisiana State University
Baton Rouge, USA
iyengar@bit.csc.lsu.edu

Abstract

Land surface temperature mapping is one of the key parameters in the physics of land surface processes. The present study covers recovering of land surface temperature from space. The study includes the separation of emissivity and temperature by using different methods. It includes computation of radiant and kinetic temperatures of the land features from Landsat 5 TM Thermal Infrared (TIR) data. Temperature mapping is done with Thermal Infrared (TIR) daytime and nighttime data. The mapping is also done using spatially improved daytime and nighttime data. As a final note, the findings between the use of improved TIR data and raw TIR data are compared and discussed.

1. Introduction

Temperature mapping is one of the major applications of the thermal infrared remote sensing. The Thermal Infrared (TIR) images are interpreted for various purposes such rock type discrimination, mapping of geological structures (Faults Zones), and mapping of surface moisture [3]. The interpretation of TIR imageries using digital image analysis includes Temperature Mapping, Image Enhancement, and Classification [5]. Multi-spectral image classification was previously carried out using visible and near infrared data along with daytime and nighttime thermal infrared data using Maximum Likelihood and Artificial Neural Networks (ANN) approaches [1,6]. It can also be done using spatially improved TIR data [12]. In the present paper, temperature mapping using raw and improved thermal infrared data are studied. Landsat 5-TM data of bands 2, 3, 4 at 30m spatial resolution, band 6 (TIR) daytime data at 120m spatial resolution and nighttime data at 120m spatial resolution acquired on 20th Dec 1989 were used in the studies [7].

Land surface temperature mapping is one of the main applications of the thermal infrared remote sensing. It involves derivation of *radiant temperatures* from digital numbers of TIR data. *Kinetic temperatures* are then calculated from radiant temperatures using the emissivity values of land-use classes. For this, classification was done using Artificial Neural Networks [6] and emissivity values [4,10] were assigned for each land-use classes. With improved spatial resolution of TIR data it is expected that results of temperature mapping will also be improved. Therefore, in the present study, improved TIR data is used for temperature mapping and the results were compared with those using raw TIR data. The details of the studies carried out on temperature mapping using Landsat 5 TM thermal infrared data and improved TIR data are presented in detail.

2. Related Research

Peter and Simon [13] conducted a study on the accuracy of three techniques for recovering surface kinetic temperature from multispectral thermal infrared data acquired over land. They found that emissivity normalization and alpha emissivity techniques are the most accurate, and recover the temperature of the majority of the artificial radiance spectra to within 1.5 °K, and the reference channel method producing less accurate results. Wan and Dozier [2,16] made an attempt to apply multiple wavelength (split window) method to measure the land surface temperature. Actually split window method is used to measure sea-surface temperatures. Previously Price [9,10] worked on the same problem and found that variations in the spectral emissivity produce large errors in temperature calculations. Wan and Dozier [16] found several reasons for unacceptable errors during the land surface temperature by applying the split window technique.

Prakash et al., [8] developed a method for coal fire detection using Landsat 5 TM thermal infrared data. Zhang et al., [15] carried out a study on the same method and he proposed a new method to evaluate the capability of Landsat-5 TM band 6 data for sub-pixel coal fire detection. Sub-pixel problem arises when the size of coal fires is less than the IFOV (instantaneous field of view) of TM on board Landsat 5, channel-6. Zhang adopted the

same method, which was used by Robinson [11]. From the analysis of results he found that Landsat TM nighttime data is still coarse in spatial resolution. Also he concluded that with knowledge of infrared scanner data or field survey data, the temperature of coal fire could be estimated. For generating thermal maps of surface temperatures many procedures are available in literature. In each case they assume that they are dealing with temperature mapping of water bodies so as to eliminate the problem of considering emissivities of different objects, which is required for mapping terrestrial temperatures. In thermal infrared remote sensing, radiation emitted by ground objects can be measured for temperature estimation. If the amount of radiation emitted from the ground can be measured by a remote sensor then the ground temperature can be estimated using Planck's equation. Prakash et al., [8] used the equations developed by NASA for estimating ground temperatures from Landsat 5 TM band 6 TIR Image. In the present study the same process is adopted.

3. Study Area

The study was performed on the area around the Thane creek with the suburban of North Mumbai, which consists of thick vegetation, forests, lakes, swamps, barren lands, hills, urban mixed areas etc. Landsat-5 TM, band 6 (TIR) daytime data at 120m spatial resolution and band 2, 3, 4 data at 30m spatial resolution, acquired on 20th Dec., 1989 and TIR night-time data at 120 m resolution acquired on 20th Dec 1989, were available and used for the studies. The bands 2, 3 and 4 data was used in deriving a False Color Composite–FCC and used as a ground truth base map.

4. Computation Of Radiant Temperatures

The method proposed by Markham and Barker [14] is used in estimating the radiant temperatures from the digital number (DN) values of TIR data, knowing the emissivity values of the classes, and in calculating kinetic temperatures. This method was adopted by Prakash et al., [8] to detect the surface coal fires of Jharia coalfields and the same method is also used in the present study for temperature mapping. Spectral radiance of earth surface features is given by Planck's equation.

Landsat-5 TM band 6 digital number values are converted into spectral radiance values using equation 1, (Markham and Barker, [14]).

$$L_\lambda = L_{MIN} + \left[\frac{L_{MAX} - L_{MIN}}{Q_{CAL\,MAX}} \right] Q_{cal} \qquad [1]$$

L_λ is the spectral radiance received by the sensor for pixel in question.

L_{MIN} is the minimum detected spectral radiance. ($0.1238 \text{mWcm}^{-2} \text{ sr}^{-1} \text{ μm}^{-1}$)

L_{MAX} is the maximum detected spectral radiance. ($1.56 \text{mWcm}^{-2} \text{ sr}^{-1} \text{ μm}^{-1}$)

$Q_{CAL\,MAX}$ is the maximum gray level (255),

Q_{CAL} is the Grey level for the analyzed pixel.

Maximum (L_{MAX}) and minimum (L_{MIN}) spectral radiance values (Table 1) for the Landsat 5 TM band 6 are taken from Landsat technical notes (1986). The radiant temperatures (T_r) are computed from spectral radiance (L_λ) by the following equation 2.

$$T_R = \frac{K_2}{\ln\left[\frac{K_1}{L_\lambda} + 1 \right]} \qquad [2]$$

T_R is Radiant Temperature in °K for pixel in question.

K_1 is calibration constant (60.776 mWcm^{-2} sr^{-1} μm^{-1})

K_2 is calibration constant (1260.56 K)

Table 1. Landsat TM spectral radiances, L$_{MIN}$ and L$_{MAX,}$ in (mWcm^{-2} sr^{-1} μm^{-1}) (Source: Landsat Technical Notes, 1986)

	Prior to 15 Jan 1984 (TIPS-ERA Processing)		After 15 Jan 1984 (TIPS-ERA Processing)	
Band	L$_{MIN}$	L$_{MAX}$	L$_{MIN}$	L$_{MAX}$
TM 1	0.000	14.28	-0.15	15.21
TM 2	0.000	29.12	-0.28	29.68
TM 3	0.000	22.50	-0.12	20.43
TM 4	0.000	21.42	-0.15	20.62
TM 5	0.000	3.000	-0.037	2.719
TM 6	0.484	1.240	0.1238	1.560
TM 7	0.000	1.593	-0.015	1.438

5. Derivation of Landuse Classes

In order to assign the correct emissivity values for different ground objects a classified image is required. A classified image is derived using Landsat TM band 2, 3, 4 and 6 images by Artificial Neural Networks approach. Emissivity values (Table 2) are assigned appropriately to all the classes. These emissivity values are used along with thermal infrared image for land surface temperature mapping.

Table 2. Emissivity values of different classes

Class Name	Emissivity
Thick vegetation	0.940
Light vegetation	0.925
Marshy land	0.950
Pure water	0.980
Turbid water	0.962
Built Up land	0.925
Open ground	0.920

6. Computation of Kinetic Temperatures

Kinetic temperatures T_K are computed from derived radiant temperatures T_R. Emissivity values are required to convert the radiant temperatures into the kinetic temperatures. Equation 3 shows the relation between the radiant temperature, kinetic temperature and the emissivity. Steps involved in this method are given in the figure 1.

$$T_R = \varepsilon^{1/4}\ T_K \qquad\qquad [3]$$

Fig 1. Flowchart of Temperature Mapping
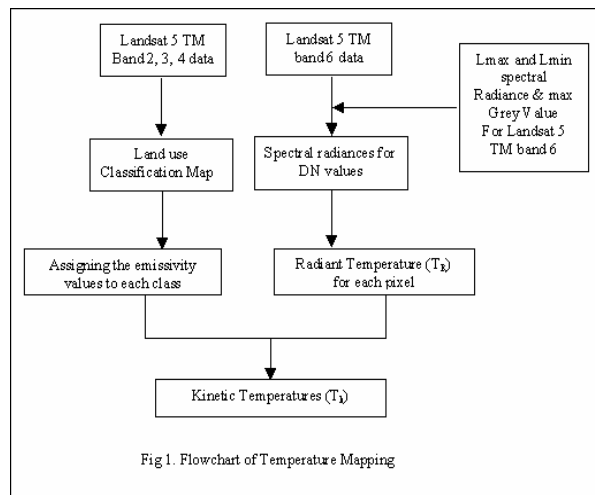
7. Test Results

In the present study, radiant temperature mapping and kinetic temperature mapping was performed for the following data:

1. Daytime raw thermal data.
2. ANN improved daytime thermal infrared image (IDTI3-using 3 bands).
3. Radiant temperature mapping using ANN improved daytime thermal infrared image (IDTI4-using 4 bands).
4. Nighttime raw thermal infrared data.
5. ANN improved nighttime thermal infrared image (INTI3-using 3 bands).
6. ANN improved nighttime thermal infrared image (INTI4-using 4 bands).

Temperature ranges for all the classes for daytime TIR image are tabulated in the tables 3 to 5. For each class, temperatures are changing by 4-5° between the raw thermal image and improved thermal image. Only for Thick vegetation the change is maximum by 7-8°.

Table 3. Temperature mapping using raw daytime thermal infrared image

Class Name	Radiant Temp. (°C)		Kinetic Temp. (°C)	
	Max	Min	Max	Min
Thick Veg.	42.00	19.03	44.67	21.07
Light Veg.	33.28	19.94	34.83	21.43
Marshy land	39.68	19.03	46.07	25.18
Pure water	37.31	18.12	42.15	22.65
Turbid water	42.00	**17.19**	46.07	**20.94**
Built Up land	43.53	19.03	**51.08**	26.00
Open ground	**43.53**	19.94	49.76	25.71

Table 4. Temperature mapping using ANN improved day TIR image (IDTI3)

Class Name	Radiant Temp. (°C)		Kinetic Temp. (°C)	
	Max	Min	Max	Min
Thick Veg.	33.69	24.40	35.45	26.89
Light Veg.	37.71	24.40	39.28	25.91
Marshy land	27.43	22.19	33.76	28.41
Pure water	29.55	**20.85**	34.27	**25.43**
Turbid water	38.10	21.75	42.12	25.55
Built Up land	40.84	25.71	48.33	32.83
Open ground	**43.15**	23.52	**49.37**	29.36

Table 5. Temperature mapping using ANN improved day TIR image (IDTI4)

Class Name	Radiant Temp. (°C)		Kinetic Temp. (°C)	
	Max	Min	Max	Min
Thick Veg.	33.28	25.71	35.45	27.67
Light Veg.	35.71	26.57	37.28	28.09
Marshy land	33.39	24.40	36.78	30.67
Pure water	33.80	**23.96**	35.54	**25.43**
Turbid water	40.07	24.40	44.11	25.55
Built Up land	41.62	27.00	**49.12**	32.83
Open ground	**42.39**	24.40	48.59	29.36

Temperature ranges for all the classes for nighttime TIR image are tabulated in the tables 6 to 8. For each class temperatures changes for nighttime images is little more than daytime results, by 5-6˚ between the raw thermal image and improved thermal image.

Table 6. Temperature mapping using raw nighttime TIR image

Class Name	Radiant Temp. (°C)		Kinetic Temp. (°C)	
	Max	Min	Max	Min
Thick Veg.	20.85	**5.97**	22.34	**7.39**
Light Veg.	17.19	6.49	23.30	12.37
Marshy land	19.94	6.49	24.51	10.84
Pure water	20.85	8.51	27.04	14.44
Turbid water	**21.75**	9.01	**28.78**	15.74
Built Up land	20.85	5.97	26.63	11.47
Open ground	19.94	5.97	25.31	11.08

Table 7. Temperature Mapping for ANN improved nighttime TIR image (INTI3)

Class Name	Radiant Temp. (°C)		Kinetic Temp. (°C)	
	Max	Min	Max	Min
Thick Veg.	13.41	8.01	14.86	**9.43**
Light Veg.	10.99	9.01	16.97	14.95
Marshy land	14.37	9.51	18.82	13.91
Pure water	14.37	8.51	20.42	14.44
Turbid water	15.79	7.50	22.68	14.20
Built Up land	**17.65**	5.97	**23.37**	11.47
Open ground	12.45	**7.00**	17.68	12.12

Table 8. Temperature mapping using ANN improved nighttime TIR image (INTI4)

Class Name	Radiant Temp. (°C)		Kinetic Temp. (°C)	
	Max	Min	Max	Min
Thick Veg.	11.97	7.50	13.41	**8.92**
Light Veg.	10.00	8.51	15.97	14.44
Marshy land	12.93	9.01	17.39	13.41
Pure water	12.45	7.50	18.46	13.41
Turbid water	**13.41**	7.00	**20.25**	13.68
Built Up land	13.41	5.97	19.05	11.47
Open ground	12.45	**6.49**	17.68	11.60

8. Comparison of Results

Temperature mapping is done by converting Landsat5 TM band6 digital number values to spectral radiance values and then into radiant temperatures. With the known emissivity values for the different classes, kinetic temperatures are estimated from the radiant temperatures. In order to assign the emissivity values to each class, classified images were produced by ANN method using Landsat 5 TM multi-spectral data (band 2, 3, 4 and 6). Radiant temperature map and kinetic temperature maps of raw daytime TIR data are obtained with the above procedure are shown in the figures 2 and 3. Radiant temperature ranged from 17˚ to 44˚ whereas kinetic temperatures ranged from 20˚ to 51˚ in the raw daytime TIR data (Table 3).
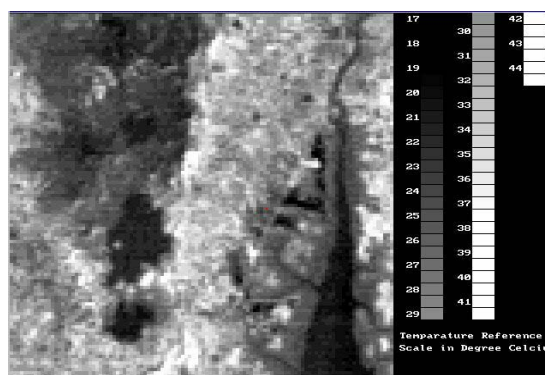

Figure 2. Radiant temperature mapping of daytime raw thermal data

Figure 3. Kinetic temperature mapping of daytime raw thermal data

Radiant temperature map and kinetic temperature maps of improved daytime TIR data (IDTI3) by ANN are shown in the figures 4 and 5. Radiant temperatures ranged from 20˚ to 44˚ whereas kinetic temperatures ranged from 25˚ to 50˚ in the improved daytime TIR data (IDTI3) by ANN (Table 4).
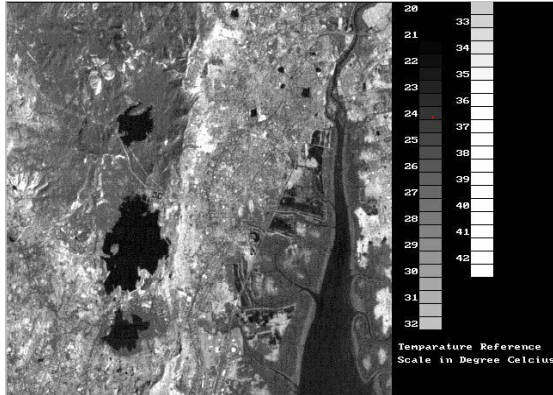
Figure 4. Radiant temperature mapping using ANN improved daytime TIR image (IDTI3)
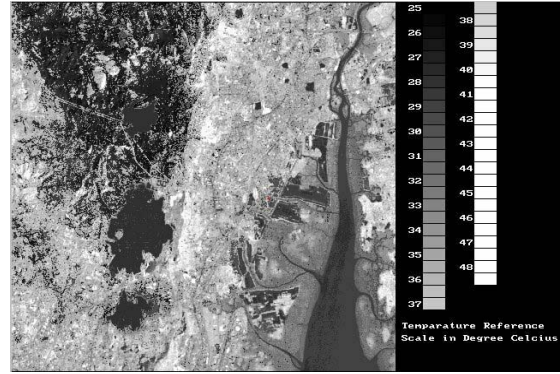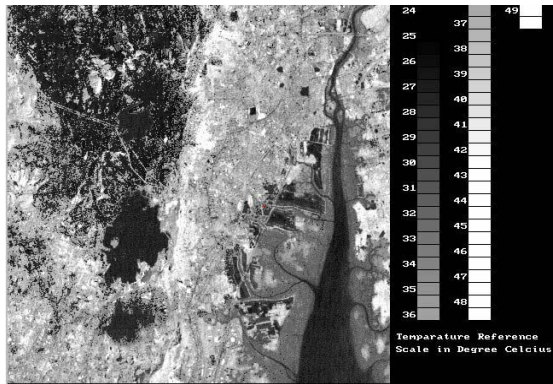

Figure 5. Kinetic temperature mapping using ANN improved daytime TIR image(IDTI3)

Radiant temperature map and kinetic temperature maps of improved daytime TIR data (IDTI4) by ANN are shown in the figures 6 and 7. Radiant temperatures ranged from 23° to 43° whereas kinetic temperatures ranged from 25° to 50° in the improved daytime TIR data (IDTI4) by ANN (Table 5).

Figure 6. Radiant temperature mapping using ANN improved daytime TIR image(IDTI4)

Figure 7. Kinetic temperature mapping using ANN improved daytime TIR image (IDTI4)

There is a change of 4°-5° between the temperatures calculated from the original daytime data and improved daytime data of the objects. Radiant temperature map and kinetic temperature maps of raw nighttime TIR data are shown in the figures 8 and 9. Radiant temperature ranged from 6° to 22° whereas kinetic temperatures ranged from 7° to 29° in the raw nighttime TIR data (Table 6).
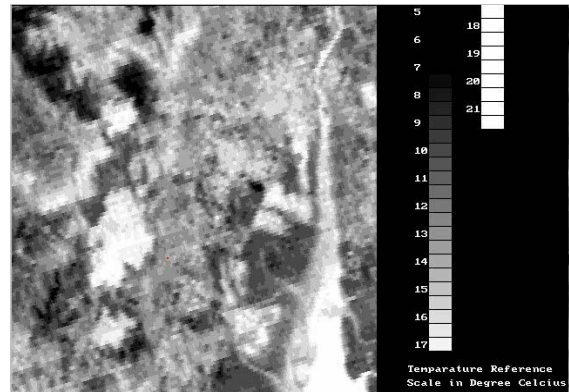

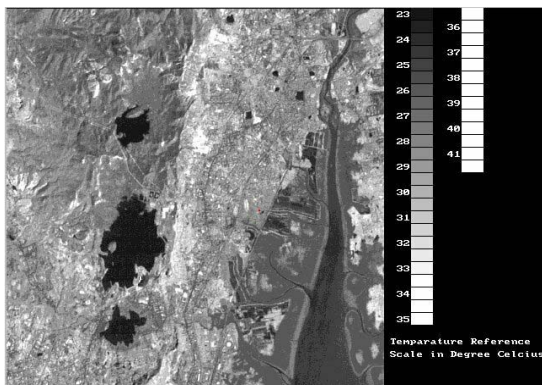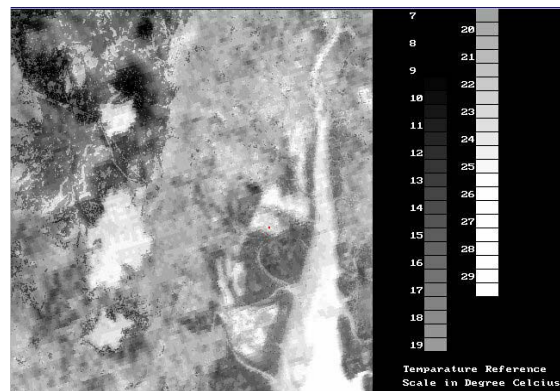**Figure 8. Radiant temperature mapping of nighttime raw TIR data**

Figure 9. Kinetic temperature mapping of nighttime raw thermal data

IEEE
COMPUTER
SOCIETY

Radiant temperature map and kinetic temperature maps of improved nighttime TIR data (INTI3) by ANN are shown in the figures 10 and 11. Radiant temperatures ranged from 7° to 18° whereas kinetic temperatures ranged from 9° to 24° in the improved nighttime TIR data (INTI3) by ANN (Table 7).
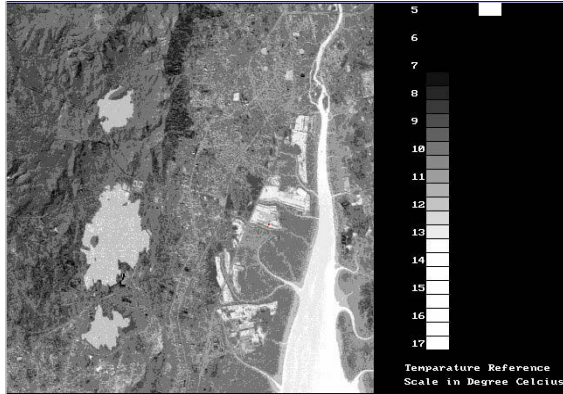

Figure 10. Radiant temperature mapping using ANN improved nighttime TIR image (INTI3)
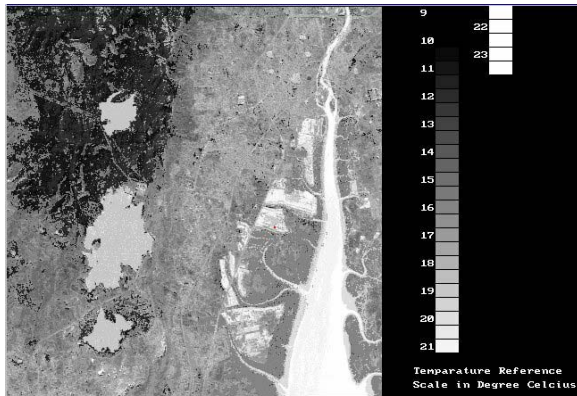

Figure 11. Kinetic temperature mapping using ANN improved nighttime TIR image (INTI3)

Radiant temperature map and kinetic temperature maps of improved nighttime TIR data (INTI4) by ANN are shown in the figures 12 and 13. Radiant temperatures ranged from 6° to 13° whereas kinetic temperatures ranged from 9° to 21° in the improved nighttime TIR data (INTI4) by ANN (Table 8).
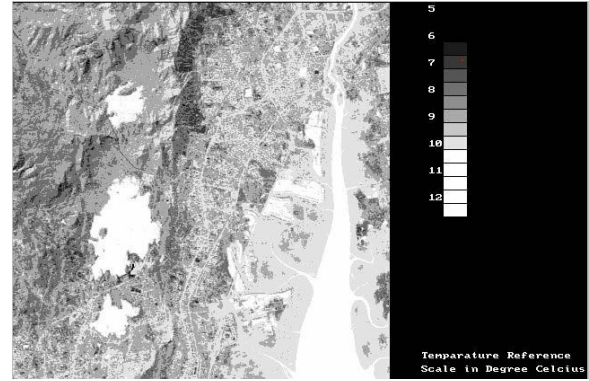

Figure 12. Radiant temperature mapping using ANN improved nighttime TIR image (INTI4)
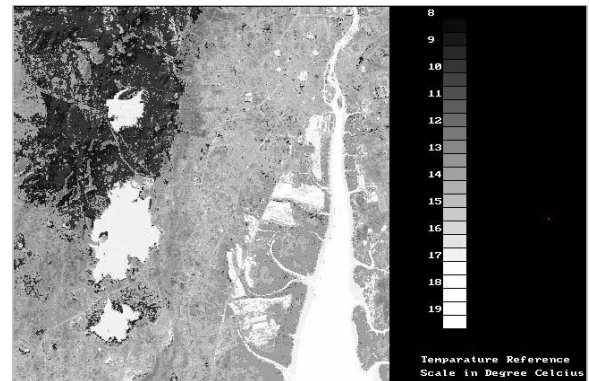

Figure 13. Kinetic temperature mapping using ANN improved nighttime TIR image (INTI4)

There is a change of 5°- 6° between the temperatures calculated from the original nighttime data and improved nighttime data of the objects.

9. Conclusions

Land surface temperature mapping using thermal infrared images is the main objective of this study. From the analysis of the results of the present study the following conclusions are drawn:

1. Estimation of temperatures using raw thermal infrared image are found to be reasonable but ground truth is essential for verification.
2. Accuracy of the temperature mapping depends on the accuracy of the classified image and the accurate emissivity values chosen for different classes. Especially in highly mixed urban areas it is difficult to assign proper emissivity values to each class.

In this study, we have demonstrated the details of temperature mapping on using raw and improved thermal infrared data. There was a change of 4°-5° and a change of 5°- 6° between the temperatures calculated from the

original/raw daytime data and improved daytime data of the objects and between the temperatures calculated from orginal/raw nightime data and improved nighttime data respectively.

10. References

[1] Benediktsson, J.A., and Sveinson, J.R., 'Feature extraction for multisource data classification with Artificial Neural networks', *International Journal of Remote sensing,* Vol.18, N0.4, pp.727-740, 1997.

[2] Dozier, J. 'A Method of Satellite Identification of Surface Temperature Fields of Subpixel Resolution'. *Remote Sensing of Environment*, Vol-11, pp. 221-229, 1981.

[3] Elachi Charles, '*Introduction To Physics And Techniques of Remote Sensing'*. John Wiley & Sons, 1987.

[4] Labed J., And M. P. Stoll 'Spatial Variability of Land Surface Emissivity In The Thermal Infrared Band: Spectral Signature And Effective Surface Temperature'. *Remote Sensing of Environment ,* Vol. 38 , No 11, pp. 1-17, 1991.

[5] Lillesand M. Thomas And Kiefer W. Ralph '*Remote Sensing And Image Interpretation'.* Third Edition. John Wiley & Sons, Inc, 1994.

[6] Venkateshwarlu, C., Gopal Rao, K., and Prakash, A., 2003, Artificial neural networks in the improvement of effective spatial resolution of thermal infrared data for improved landuse classification", URBAN-2003: Second IEEE/ISPRS Joint Workshop on Remote Sensing and Data Fusion over Urban Areas, May 22-23, Berlin, Germany.

[7] Ormsbay P. James, 'The Use of Landsat-3 Thermal Data to Help Differentiate Land Covers'. *Remote sensing of environment*, vol-12, pp. 92-105, 1982.

[8] Prakash, A., Saraf, A. K., Sengupta S., and Gupta, R. P. 'Landsat TM Data For Estimating Ground Temperature and Depth of Subsurface Coal Fires in Jharia Coal Field, India'. *International Journal of Remote Sensing,* Vol-16, No.12, pp. 2111-2124, 1995.

[9] Price C. John 'The Contribution of Thermal Data in Landsat Multi Spectral Classification'. *Photogrammetric Engineering and Remote Sensing*, Vol-47, No-2, pp. 229-236, 1981.

[10] Price C. John 'Estimating Surface Temperature From Satellite Thermal Infrared Data - A Simple Formulation for The Atmospheric Effect'. *Remote Sensing of Environment*, Vol-13, pp. 353-361, 1983.

[11] Robinson, J.M. 'Fire From Space: Global Fire Evaluation Using Infrared Remote Sensing'. *International Journal of Remote Sensing*, Vol-12, pp. 3-24, 1991.

[12] Sabins F. Floyd '*Remote Sensing Principles and Interpretation'*, Third Edition. W. H. Freeman and Company, New York, 1997.

[13] Peter S. Kealy And Simon J. Hook 'Separating Temperature And Emissivity In Thermal Infrared Multispectral Scanner Data: Implication For Recovering Land Surface Temperatures'. *IEEE Transactions on Geosciences and Remote Sensing*, Vol-31, No-6, pp.1155-1164, 1993.

[14] Markham, B., and Barkher, J.L.,'Spectral Characterization of Landsat Thematic Mapper Sensors', *International Journal of Remote Sensing*, 1998, Vol-6, pp. 697-716, 1985

[15] Xiangmin Zhang, J.L.Van Gendern And S.B.Kroonenberg 'A Method To Evaluate The Capability of Landsat TM Band 6 Data For Sub-pixel Coal Fire Detection'. *International Journal of Remote Sensing*, 1997, Vol-15, pp. 3279-3288, 1997.

[16] Zhengming Wan and Jeff Dozier 'Land Surface Temperature Measurement From Space : Physical Principles And Inverse Modeling'. *IEEE Transactions on Geosciences and Remote Sensing,* May 1989, Vol. 27, No 3, pp. 268-277, 1989.